Mean-field model of the Verwey transition in magnetite

Ricardo Aragón and Jurgen M. Honig
Department of Chemistry, Purdue University, West Lafayette, Indiana 47907-3699
(Received 6 July 1987)

A mean-field model is applied to the Verwey transition in $Fe_{3(1-\delta)}O_4$. Parametrization of the internal energy, in terms of the experimental dependence of transition temperature on metal-oxygen nonstoichiometry, yields results consistent with the existence of two regimes on either side of a critical composition $\delta_c=0.0039$. For $\delta<\delta_c$, first-order transitions occur, with singlet ground states and doublet excited states. For $\delta>\delta_c$, second-order transitions result, for ground and excited states of equal degeneracy. The density of states, determined by a single long-range-order parameter is used to calculate the Fermi potential of a free-electron gas and associated electrical transport properties, as a function of temperature and nonstoichiometry. The canonical cusp catastrophe describes critical behavior in the mean-field approximation.

I. INTRODUCTION

The Verwey[1] transition of magnetite has received widespread attention in the last five decades, motivated by interest in its typicality as a critical phenomenon, as well as in associated physical properties of fundamental and technological significance.

In common with all mixed-valence compounds, most physical properties are profoundly influenced by changes of concentration in cation oxidation states, associated with departures from ideal metal-oxygen stoichiometry, in the case of transition-metal oxides. Accordingly, recent systematic investigations[2] of the influence of nonstoichiometry on magnetite have revealed additional experimental results, most dramatically illustrated by the sudden change in the order of the transition,[3] beyond a critical level of cation deficiency.

The mean-field approximation provides a convenient framework, in which these new observations may be interpreted, with a minimum number of adjustable parameters. The ensuing description is not limited to the fitting of experimental data to a heuristic equation of state, providing, rather, some insight into physical behavior, on which more realistic models may be based.

It has long been recognized[4] that all the interesting physics in the canonical partition function is contained in the density of states, since the exponential is a monotonically decreasing function. In 1965, Strässler and Kittel[5] provided an elementary analysis of the conditions for phase transitions, affecting interacting systems in the molecular field approximation, in which a minimum requirement of two possible microstates[6] yields very simple closed form expressions for the density of states, which are the basis of the present work.

II. REVIEW OF THE STRÄSSLER AND KITTEL (REF. 5) FORMALISM

Given a large number N of identical subsystems, with ground state at energy zero and degeneracy g_0 and an excited state at energy ϵ of degeneracy g_1, the state of the system is described by the single long-range-order parameter:

$$\psi=\frac{n_1}{N}\ , \tag{1}$$

where n_1 excited subsystems can be distributed in

$$g_1^{n_1}g_0^{N-n_1}\frac{N!}{n_1!(N-n_1)!}$$

independent arrangements. With the Stirling approximation, the entropy $S(\psi)$ is

$$S(\psi)=N[\psi\ln g_1+(1-\psi)\ln g_0-\psi\ln\psi -(1-\psi)\ln(1-\psi)]\ . \tag{2}$$

Consistently with mean-field theories, the harmonic approximation is introduced, to truncate the Taylor expansion of the internal energy (U) at the quadratic term, such that

$$U=N(\epsilon\psi-\tfrac{1}{2}\lambda\psi^2)\ , \tag{3}$$

where λ is a positive constant, which accounts for all interactions. Assuming $\epsilon\geq\lambda/2$, the ground state corresponds to $\psi=0$.

The free energy per subsystem is

$$F=\frac{U-kTS}{N}=\epsilon\psi-\tfrac{1}{2}\lambda\psi^2 -kT[\psi\ln g_1+(1-\psi)\ln g_0-\psi\ln\psi -(1-\psi)\ln(1-\psi)]\ , \tag{4}$$

by substitution of Eqs. (2) and (3), where k_B is Boltzmann's constant.

Application of the equilibrium constraint $\partial F/\partial\psi=0$ yields the equation of state

$$\epsilon-\lambda\psi-k_BT\left[\ln\left[\frac{g_1}{g_0}\right]+\ln\left[\frac{1-\psi}{\psi}\right]\right]=0\ . \tag{5}$$

The conditions for the existence of first- or second-order transitions, at the temperature T_V, can be derived in the usual manner, by the introduction of appropriate constraints on the higher-order derivatives of the free energy.

(a) *Second-order transitions* require at T_V

$$F'=F''=F'''=0 \quad \text{and} \quad F^{\mathrm{IV}}>0\ . \tag{6}$$

Since

$$\frac{\partial^3 F}{\partial\psi^3}=-k_BT\left[\frac{1}{\psi^2}-\frac{1}{(1-\psi)^2}\right], \tag{7}$$

it can vanish only if $\psi=1-\psi=\frac{1}{2}$. Substitution in Eq. (5) yields

$$\lambda=4k_BT_V\ , \tag{8}$$

$$\epsilon=\left[2+\ln\left[\frac{g_1}{g_0}\right]\right]k_BT_V\ , \tag{9}$$

$$\epsilon/\lambda=\tfrac{1}{2}+\tfrac{1}{4}\ln(g_1/g_0)\ . \tag{10}$$

(b) *First-order transitions* occur at T_V if there exist two values ψ_1 and ψ_2 for which

$$\begin{aligned}&F(\psi_1)=F(\psi_2),\quad F'(\psi_1)=F'(\psi_2)=0\ ,\\ &F''(\psi_1)>0 \quad \text{and} \quad F''(\psi_2)>0\ .\end{aligned} \tag{11}$$

These conditions can be met only if ψ_1 and ψ_2 provide symmetric solutions of Eq. (5) about $\psi=\frac{1}{2}$, which requires that

$$\epsilon-\lambda/2=k_BT_V\ln(g_1/g_0)\ . \tag{12}$$

In addition, F must have a maximum at $\psi=\frac{1}{2}$; therefore,

$$\frac{\partial^2 F}{\partial\psi^2}=-\lambda+k_BT_V\frac{1}{\psi(1-\psi)} \tag{13}$$

must be negative at $\psi=\frac{1}{2}$ or, equivalently,

$$\lambda>4k_BT_V\ . \tag{14}$$

It follows from (11) and (13) that

$$\epsilon/\lambda<\tfrac{1}{2}+\tfrac{1}{4}\ln(g_1/g_0)\ , \tag{15}$$

and $g_1>g_0$.

The ratio ϵ/λ is, therefore, the discriminant for first- or second-order character of the transition.

III. ANALYSIS BY CATASTROPHE THEORY

There are conceptual advantages in examining the Strässler and Kittel potential in terms of catastrophe theory, in order to describe the manner in which changes of the internal energy parameters ϵ and λ, which are functions of chemical composition, influence the character of the transition.

In $Fe_{3(1-\delta)}O_4$, a critical[3] composition δ_c exists, for which the transition changes from first to second order, of coordinates[7] T_c, the transition temperature for this composition, ϵ_c and λ_c, the values of the internal energy parameters, which by Eqs. (8), (9), (14), and (15) should correspond to their lower limits:

$$\epsilon_c=[2+\ln(g_1/g_0)]k_BT_c \quad \text{and} \quad \lambda_c=4k_BT_c\ , \tag{16}$$

and ψ_c, the critical value of the order parameter, which must be $\frac{1}{2}$ by the arguments leading to Eqs. (8) and (12).

The internal energy parameters are expressed in units of thermal energy and, following standard procedure, the reduced variables are defined with a shift of the origin to the critical point. Consequently, the control variables are

$$e=\frac{\epsilon/k_BT}{\epsilon_c/k_BT_c}-1=\frac{\epsilon}{k_BT[2+\ln(g_1/g_0)]}-1\ , \tag{17}$$

$$l=\frac{\lambda/k_BT}{\lambda_c/k_BT_c}-1=\frac{\lambda}{4k_BT}-1\ , \tag{18}$$

and the essential variable is

$$r=\frac{\psi}{1/2}-1=2\psi-1\ . \tag{19}$$

For a single essential variable, the characterization of the appropriate unfoldings may be obtained either from the potential expansion or from its gradient, the equation of state, with equivalent results.[8]

A. Standard form of the catastrophe manifold

Division of the equation of state (5) by k_BT and substitution of the reduced variables yields

$$e[2+\ln(g_1/g_0)]-2l-2(l+1)r+\ln\left[\frac{1+r}{1-r}\right]=0\ , \tag{20}$$

and its Taylor expansion around the origin, divided by 2, is

$$e[1+\tfrac{1}{2}\ln(g_1/g_0)]-l(1+r)+\frac{r^3}{3}+\frac{r^5}{5}+\cdots=0\ . \tag{21}$$

At the origin, $e=l=0$, the first noncanceling term is $r^3/3$, which makes the unfolding $f(r)$ strongly three-determinate[9] and, consequently, strongly equivalent to a cubic truncation.[10] A smooth change of variables exists, such that the mapping to the standard form is[11]

$$r^3-3lr+3\{e[1+\tfrac{1}{2}\ln(g_1/g_0)]-l\}=0\ , \tag{22}$$

which is readily recognized as the canonical expression for the *cusp* catastrophe manifold.

B. Standard form of the potential unfolding

The mapping of the free-energy potential follows by the same methods applied to the equation of state. The free-energy potential [Eq. (4)], expressed in units of $k_BT/2$, in terms of the reduced variables, is

$$F\frac{2}{k_BT}=[2+\ln(g_1/g_0)](e+1)(r+1)-(l+1)(r+1)^2-r\ln(g_1/g_0)+\ln[(r+1)(1-r)]$$
$$+r\ln\left[\frac{r+1}{1-r}\right]-\ln(g_1g_0)-2\ln 2\ , \tag{23}$$

and its Taylor expansion around the origin is

$$F\frac{2}{k_BT}=[2+\ln(g_1/g_0)](e+1)-(l+1)-\ln(g_1g_0)-2\ln 2$$
$$+\{[2+\ln(g_1/g_0)](e+1)-2(l+1)-\ln(g_1/g_0)\}r-lr^2+\tfrac{1}{6}r^4+\tfrac{1}{15}r^6+\cdots\ . \tag{24}$$

The algebraic sum of all terms independent of r, known as the shear term, has no influence on critical behavior and may be omitted from the relevant potential Φ, obtained from Eq. (24), by multiplication by a scaling factor of $\frac{3}{2}$:

$$\Phi=3\{[1+\tfrac{1}{2}\ln(g_1/g_0)]e-l\}r-\tfrac{3}{2}lr^2+\tfrac{1}{4}r^4+\tfrac{1}{10}r^6+\cdots\ . \tag{25}$$

The same analysis used on Eq. (21) proves the potential at the origin, Φ_{00} ($e=l=0$), to be strongly four-determinate and, consequently, strongly equivalent to a fourth-order truncation:[12]

$$\tfrac{1}{4}r^4-\tfrac{3}{2}lr^2+3\{[1+\tfrac{1}{2}\ln(g_1/g_0)]e-l\}r\ , \tag{26}$$

which has the form of the standard cusp-potential unfolding. It is readily verified that its derivative with respect to r, yields the cusp-catastrophe manifold [Eq. (22)].

C. Significance of the cusp catastrophe

The mapping of the Strässler and Kittel potential onto a cusp catastrophe is assured by Thom's theorem[13] of elementary catastrophes. It is sufficient to recognize in the free-energy expression (4) the existence of a single essential variable and two controls, which fix the co-rank and co-dimension at 1 and 2, respectively; four-determinacy is the only possible result. This is a direct consequence of the mean-field approximation introduced in Eq. (3), where the Taylor expansion of the internal energy was truncated in the quadratic term. Its Legendre transform, namely the free-energy expression (4), is the equation of the tangent hyperplanes to its graph with manifest singularity. The cusp character is therefore determined by the chosen internal energy function and transferred by virtue of the equivalence of Legendre invariance and catastrophe invariance.[14]

All the information obtainable from a mean-field model may be derived from inspection of the potential[15] [Eq. (26)]. The relevant features are best summarized by a three-dimensional plot of the catastrophe manifold [Eq. (22)] and its projections (see Fig. 1).

A section of the cusp along its major axis yields the parabolic Maxwell coexistence curve of solutions for two identical minima of $\frac{1}{4}r^4-\frac{3}{2}lr^2$, which corresponds to the critical exponent value $\frac{1}{2}$, characteristic of mean-field theories.

The projection onto the control space yields the bifurcation set of the cusp, solutions to the semicubical parabola:

$$-4l^3+9\{[1+\tfrac{1}{2}\ln(g_1/g_0)]e-l\}^2=0\ . \tag{27}$$

This analysis is entirely analogous to the description of criticality in a van der Waals fluid.[16]

The major axis of the bifurcation set, $-3l$, provides the direction in which the Maxwell set of first-order transitions leaves the "pucker" or cusp point, where an isolated second-order transition occurs. Since the points on this axis correspond to

$$[1+\tfrac{1}{2}\ln(g_1/g_0)]e-l=0\ ,$$

it is easily verified that, in terms of the original coordinates, ϵ and λ, this condition corresponds to the Strässler and Kittel result for first-order transitions [cf. Eq. (12)]. A similar transformation on the minor axis

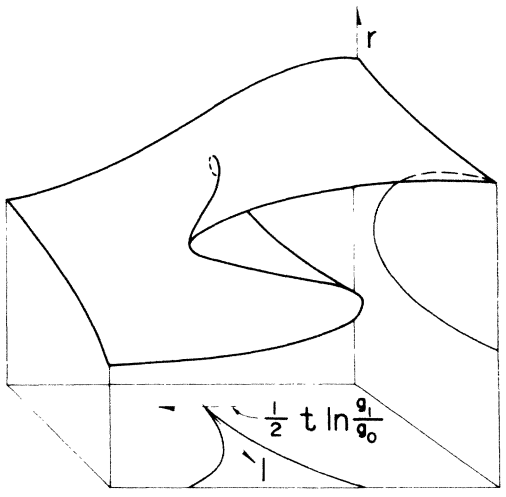

FIG. 1. Schematic drawing of the cusp catastrophe and its projections; r is the reduced order parameter $2\psi-1$; l is the reduced interaction variable $\lambda/4k_BT-1$; t is the reduced temperature $T_V/T-1$; g_0 and g_1 are the degeneracies of the ground and excited states.

shows that

$$e[1+\tfrac{1}{2}\ln(g_1/g_0)]-l=\frac{1}{2}\frac{T_V-T}{T}\ln(g_1/g_0)\ , \quad (28)$$

which represents a reduced temperature t, scaled by the logarithm of the degeneracy ratio. Consequently, the direction of the cusp pivots around the pucker point, proportionally to $\ln(g_1/g_0)$. In addition, the magnitude of the discontinuity at the transition is determined by the major-axis coordinate, gradually decreasing with diminishing interaction, until it vanishes at the cusp point, in a second-order inflection. Beyond this critical value, the interaction term is too weak to induce a transition.

If g_1 equals g_0, the third term of the potential (26), linear in r, cancels for the condition $\epsilon/\lambda=\frac{1}{2}$. The resulting unfolding is of the type $\frac{1}{4}r^4-\frac{1}{2}lr^2$, described by Poston and Stewart as "non transverse, unstable and atypical but, among even functions, the unique stable single-parameter local family around the origin."[17] The criticality observed in this case is equivalent to that of the Weiss equation of state for a ferromagnet under zero applied magnetic field.[18] The absence of a third-order invariant in the potential expansion allows the existence of contiguous second-order transitions[19] but, for the Strässler and Kittel potential, contiguity under a smooth change of control variables is possible, only if the condition on the degeneracies and the ϵ/λ ratio stated above are satisfied. Similarly, it is apparent that the absence of the cubic invariant is entirely dependent on the mean-field truncation of the internal energy expansion.

IV. APPLICATION TO THE VERWEY-TRANSITION PROBLEM

The transition temperatures, determined by relaxation calorimetry experiments on $Fe_{3(1-\delta)}O_4$ single crystals of controlled stoichiometry,[3] have been plotted as a function of δ in Fig. 2, with solid circles for first-order and open circles for second-order transitions.

Within experimental error, the data may be fitted by first-order regressions in δ, which implies that ϵ and λ may be expressed as linear functions of δ. This straight-line dependence is not guaranteed by the typicality arguments used in preceding sections, because strong equivalence preserves the direction in which the Maxwell set leaves the cusp point but not necessarily its curvature.[20] However, ϵ and λ are functions of the $[Fe^{2+}]/[Fe^{3+}]$ ratio in octahedral sites, which is linearly related to δ by preservation of electroneutrality.

The existence of a second-order regime for $\delta>\delta_c$ ($\delta_c=0.0039$) requires that $g_0=g_1$ and $\epsilon/\lambda=\frac{1}{2}$, as discussed in the preceding section. Within experimental error, the slope of the regression for the first-order regime ($\delta<\delta_c$) is ln2 times that of the second-order transitions, which is consistent with the assignment $g_1/g_0=2$, for a corresponding rotation of the Maxwell set on the control space.

The entropy of transition for the first-order regime (S_V) is easily obtained from the difference of the entropy expression [Eq. (2)], evaluated for ψ_1 and ψ_2, the magnitudes of the order parameter which satisfy conditions (11), namely

$$S_V=S(\psi_2)-S(\psi_1)=N[(\psi_2-\psi_1)\ln g_1+(\psi_1+\psi_2)\ln g_0+\psi_1\ln\psi_1-\psi_2\ln\psi_2+(1-\psi_1)\ln(1-\psi_1)-(1-\psi_2)\ln(1-\psi_2)]\ . \quad (29)$$

It is convenient to adopt the function Δ for the difference $\psi_2-\psi_1$, as defined by Strässler and Kittel:[5]

$$\psi_1\equiv\tfrac{1}{2}(1-\Delta),\quad \psi_2\equiv\tfrac{1}{2}(1+\Delta)\ . \quad (30)$$

Substitution of these definitions into Eq. (29) yields a simple expression for the entropy of transition:

$$S_V=N\Delta\ln(g_1/g_0)\ . \quad (31)$$

For stoichiometric Fe_3O_4, the experimental value for the molar entropy of transition[21] is R ln2; consequently, allowing for two octahedral sites per formula unit, $\Delta=\frac{1}{2}$ and $g_1/g_0=2$.

Strässler and Kittel[5] obtain the relation between Δ and ϵ/λ, from the difference of the ψ_1 and ψ_2 solutions to the equation of state [Eq. (5)] at the first-order transition, with the result

$$\frac{\Delta}{2\ln[(1+\Delta)/(1-\Delta)]}=\frac{k_BT_V}{\lambda}=\frac{\frac{1}{2}-\epsilon/\lambda}{\ln(g_0/g_1)}\ . \quad (32)$$

At the limit for $\Delta\to0$, the left-hand side of Eq. (32) is $\frac{1}{4}$, in agreement with Eq. (10) for a second-order transition. Regardless of the degeneracies g_1 and g_0, the value of the order parameter (ψ) above T_V for a second-order transition is fixed at $\frac{1}{2}$, as required by conditions (6) and (7).

For a first-order transition, the excitation density at infinite temperature is

$$\psi_\infty=g_1/(g_0+g_1)\ . \quad (33)$$

Substitution of this value in Eq. (32) shows that the

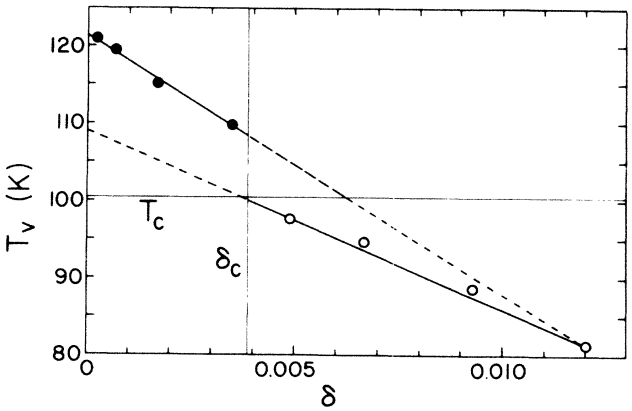

FIG. 2. Verwey-transition temperature (T_V) vs nonstoichiometry (δ) (Ref. 3). Linear regressions on first-order (solid circle) and second-order (open circle) transitions (solid lines), extrapolations (short-dashed line), and range of inaccessible normal first-order regime (long-dashed line).

value of the order parameter at the transition equals ψ_∞, if

$$\epsilon/\lambda = g_1/(g_0+g_1) . \tag{34}$$

when $\epsilon/\lambda < g_1/(g_0+g_1)$, the excitation density at the transition exceeds ψ_∞; conversely for $\epsilon/\lambda > g_1/(g_0+g_1)$, $\psi < \psi_\infty$ at all finite temperatures. Strässler and Kittel,[5] following Chesnut,[22] denote the first of these two cases as a "supertransition," and the second as an ordinary first-order transition.

Since ϵ and λ are linearly related to the transition temperature [see Eq. (12)], the experimental values of T_V at the two extremes of the first-order regime fully determine the corresponding straight-line equations. For stoichiometric magnetite, Δ equals $\frac{1}{2}$ at $T_V = 121.5$ K and Eq. (32) yields $\lambda = 4\, k_B T_V \ln 3$. Taking the second-order limit (i.e., $\Delta = 0$), at $T_V = 101$ K, with $\lambda = 4 k_B T_V$ [cf. Eq. (8)], it follows immediately that

$$\lambda_I = k_B(6.338 T_V - 236.1) , \tag{35}$$

and

$$\epsilon_I = k_B(3.862 T_V - 118.0) , \tag{36}$$

where the subscript I denotes the first-order character, in the range $121.5 \leq T_V \leq 101$.

Equation (35) may be used to obtain a numerical solution of Eq. (32) for Δ and, hence, the transition entropy [see Eq. (31)] as a function of T_V, in good agreement with the experimental results (see Fig. 3).

The change in subsystem states, which determines the character of the Verwey transition, responds to the decrease in free energy associated with a rearrangement of the energy levels. The intersection of the potential unfoldings for the respective cusps is ruled by the shear term of Eq. (24). At the cusp point (i.e., $l = e = 0$), in the second-order transition limit, the subsystems with higher ground-state degeneracy are stabilized by lower free energy. Consequently, the singlet ground-state configuration is possible only if a depression of the internal energy offsets the entropic advantage of the doublet. This requirement for the onset of the first-order transition regime can be stated in terms of the partial molal internal energy ($\bar{U}$) as

$$\bar{U} = \frac{\partial U}{\partial N\psi} = \frac{\partial}{\partial N\psi}[N(\epsilon\psi - \tfrac{1}{2}\lambda\psi^2)] = \epsilon - \lambda\psi < 0 . \tag{37}$$

At high temperature [see Eq. (33)] this limit is determined by Eq. (34). With the substitution of expressions (35) and (36), the condition $\epsilon/\lambda < \frac{2}{3}$ is satisfied by $T_V > 108.4$ K. The values $T_V = 108.4$ K and $\Delta = \frac{1}{3}$ [see Eq. (32)] at $\delta_c = 0.0039$ are lower limits for the first-order–transition regime, indicated in Fig. 3, by a change from a solid to a dashed line in the calculated entropy of transition, and correspondingly in Fig. 2 for the compositional dependence. Similarly, the intersection of the second-order regression with the extrapolation of the first order at 81 K corresponds to the lowest possible Verwey transition for $\delta = 0.012$.

In the terms used by Strässler and Kittel,[5] the two regimes observed for the Verwey transition as a function of nonstoichiometry correspond to supertransitions for $0 < \delta < 0.0039$ with $g_0 = 1$ and $g_1 = 2$, and second-order transitions with $g_0 = g_1 = 2$ for $0.0039 < \delta < 0.012$. The "normal" first-order regime is not possible. The corresponding solutions of the equation of state [see Eq. (5)] for the order parameter as a function of temperature, which are sections of the cusp-catastrophe manifold (see Fig. 1), have been plotted in Fig. 4 for each case. In this context the change from first- to second-order behavior is associated with a constraint catastrophe,[23] where the boundary $\epsilon - \lambda\psi_\infty \leq 0$ limits the domains of the interior catastrophes, excluding the topologies of Figs. 4(b) and 4(c).

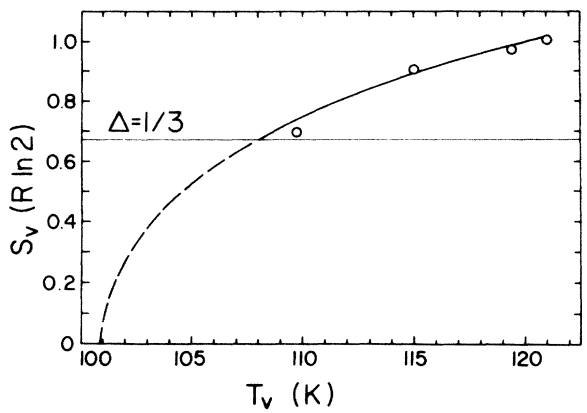

FIG. 3. Experimental entropy of transition (S_V) (Ref. 3) vs Verwey-transition temperature T_V (circles) and calculated dependence in the supertransition (solid line) and inaccessible normal first-order (dashed line) regimes.

V. ELECTRICAL TRANSPORT PROPERTIES

To the extent that the mean-field approximation is valid, the thermodynamic description presented above fully characterizes the equilibrium aspects of all physical properties of the system. Electrical transport involves this representation, because it proceeds via degenerate states restricted, in the case of magnetite, to the octahedral sublattice, which contains cations in multiple oxidation states. In this spirit, the calculations of dc electrical resistivity and Seebeck coefficient outlined in this section are intended to test the relevance of a single long-range-order parameter, to describe the thermal and composition dependence of the density of states, rather than to investigate specific transport mechanisms.

The density of states for the system follows trivially in terms of the long-range-order parameter ψ. For the excited state, at energy E_1, the probability per octahedral site is $g_1\psi$ and, for the ground state at E_0, it is $g_0(1-\psi)$. In the simplest possible approximation, these states will be populated by a noninteracting Fermi gas of electrons, with a Fermi potential η. The number of electrons in the system may be obtained from the number of ferrous cations in the generalized structural formula unit $Fe^{3+}[Fe^{3+}_{1+6\delta}Fe^{2+}_{1-9\delta}]O_4$. Consequently, the balance of carriers expression per octahedral cation has the simple form

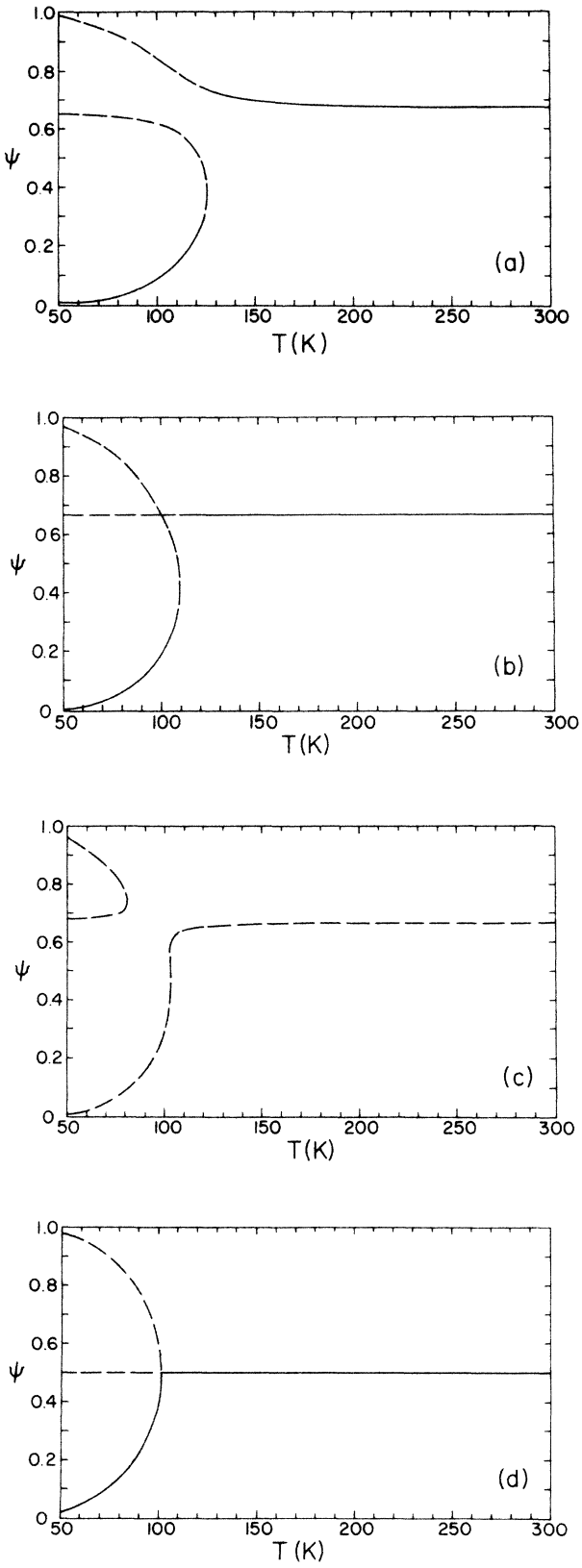

FIG. 4. Order parameter (ψ) vs temperature. (a) $\delta=0$, $T_V=121.5$ K, supertransition; (b) $\delta\rightarrow\delta_c$, $T_V=108.4$ K, "super" to normal first-order limit; (c) $T_V=103$ K, inaccessible normal first-order transition; (d) $\delta_c\leftarrow\delta$, $T_V=101$ K, second-order transition.

$$\frac{1-9\delta}{2-3\delta}=g_1\psi\frac{1}{1+\exp[(E_1-\eta)/k_BT]}+g_0(1-\psi)\frac{1}{1+\exp[(E_0-\eta)/k_BT]}\ , \tag{38}$$

where the carrier occupation of each state is obtained from the product of the probability for the state and the corresponding Fermi-Dirac statistical function.

It is appropriate to refer all energies to the energy of the transport state E_1. Accordingly, the Fermi potential is redefined as

$$\zeta\equiv E_1-\eta\ , \tag{39}$$

and the energy difference between the two states, which corresponds to the change of energy due to the excitation of one subsystem, is the partial molal internal energy:

$$E_1-E_0=\bar{U}=\epsilon-\lambda\psi \tag{40}$$

[see Eq. (37)].

The balance-of-carriers expression [Eq. (38)], with the redefined energy origin, obtained from Eqs. (39) and (40),

$$\frac{1-9\delta}{2-3\delta}=g_1\psi\frac{1}{1+\exp(-\zeta/k_BT)}+g_0(1-\psi)\frac{1}{1+\exp\{[-(\epsilon-\lambda\psi)+\zeta]/k_BT\}}\ , \tag{41}$$

can be solved numerically to obtain ζ as a function of temperature from the equilibrium value of ψ [see Eq. (5)]. For a magnetite phase of arbitrary nonstoichiometry (δ), with a transition temperature T_V, the energy parameters ϵ and λ are obtained from Eqs. (35),(36) and (8),(9) for first- (i.e., $g_1=2$, $g_0=1$) and second- (i.e., $g_1=g_0=2$) order regimes, respectively.

Emin[24] has defined the Seebeck coefficient (α) as "the change in entropy of the total system per unit charge upon adding a charge carrier." It is usually simpler to calculate the isothermal Peltier heat (π), which is[25] "the heat that must be supplied when a charge carrier is isothermally injected into a material." There are two contributions to the Peltier heat: The first, associated with placing the carrier in the material, can be calculated from equilibrium thermodynamics; the second, derived from the net energy flow in carrier motion, depends on the transport mechanism. In the adiabatic limit, the latter term cancels and Emin's[25] final expression for the Peltier heat is

$$\pi=F^1-F^0-T\frac{\partial(F^1-F^0)}{\partial T}-\eta\ . \tag{42}$$

The difference F^1-F^0, which represents "the change in free energy when a solitary carrier is added to an otherwise carrier free system," corresponds to the free energy of formation of a transport state [Eq. (4)] and is identically zero by virtue of the equilibrium condition $\partial F/\partial\psi=0$ [see Eq. (5)]. The second term of Eq. (42) is the entropic energy

$$-k_B T \ln[(g_1/g_0)(1-\psi)/\psi] ,$$

which equals $-(\epsilon-\lambda\psi)$ [see Eq. (5)], and the Fermi potential η is the solution to Eq. (38).

Numerical solutions of Eqs. (5) and (41) can be used to calculate the Seebeck coefficient from the fundamental relation $\alpha=\pi/qT$, with π determined by Eq. (42). The result for stoichiometric magnetite (i.e., $\delta=0$) has been plotted in Fig. 5(a), for comparison with the experimental data, Fig. 5(b).[26]

The fundamental expression for electrical conductivity (σ), in terms of carrier density (n), charge (e), and mobility (μ), is

$$\sigma = n_C e \mu . \tag{43}$$

The number of carriers per formula unit of $Fe_{3(1-\delta)}O_4$ is obtained directly from the first term of Eq. (41):

$$n_C = (2-3\delta) g_1 \psi \frac{1}{1+\exp(-\zeta/k_B T)} . \tag{44}$$

In the simplest possible description of electrical transport between localized states, the mobility can be modeled in the small-polaron approximation[27] as

$$\mu = (1-c) e a^2 \Gamma \frac{1}{k_B T} , \tag{45}$$

where a is the lattice constant of an fcc structure, c is the fraction of sites which contain an electron, and Γ is the jump rate of the polaron. For subsystems with only two possible states, the fraction of unoccupied transport states $(1-c)$ is equivalent to the fraction of carriers in the ground state, determined by the second term of Eq. (41), namely

$$1-c = g_0(1-\psi) \frac{1}{1+\exp\{[-(\epsilon-\lambda\psi)+\zeta]/k_B T\}} . \tag{46}$$

The jump rate of the polaron, from one site to a specific neighboring site, is generally[27] described by

$$\Gamma = P \nu_o \exp\frac{-E_H}{k_B T} , \tag{47}$$

where ν_o is the appropriate optical-mode phonon frequency, E_H is the activation energy for hopping, and P is a factor for the probability of electron transfer associated with the displacement of the polarized configuration.

Since the polaron involves the formation of a transport or excited state, the activation energy E_H may be estimated from the partial molal internal energy, in the absence of interactions:

$$E_H = \lim_{\psi\to 0} \overline{U} = \epsilon . \tag{48}$$

The probability P is a function of the time for electron transfer[27] $t_e \propto \hbar/J$, where J is the electron-transfer integral, and of the corresponding polaronic quantity: t_p. In the adiabatic limit, used in the calculation of the Seebeck coefficient, $t_e \ll t_p$, no energy is transferred, and $P \simeq 1$. If $t_e > t_p$ and $P \ll 1$ [$P \propto J^2/(k_B T)^{1/2}$], a nonadiabatic condition exists, associated with a net transfer of energy. The modeling of nonadiabatic behavior exceeds the scope of an equilibrium treatment and will not be considered further.

In the adiabatic limit, the optical frequency ν_o is the only unknown factor in the electrical conductivity expression

$$\sigma = \frac{e^2 a^2 A \nu_o}{k_B V_{\text{f.u.}}} (2-3\delta) g_1 \psi [1+\exp(-\zeta/k_B T)]^{-1} g_0 (1-\psi) \{1+\exp[(-\epsilon+\lambda\psi+\zeta)/k_B T]\}^{-1} \frac{1}{T} \exp(-\epsilon/k_B T) , \tag{49}$$

obtained by substitution of Eqs. (44)–(48) into (43), with Avogadro's number (A) and the volume per formula unit ($V_{\text{f.u.}}$) used to convert to units of carriers per unit volume.

Without further assumptions, the validity of the model may be tested by comparison with the experimental data. For this purpose, a function $R(T)$ will be defined:

$$R(T) \equiv \frac{T \exp(\epsilon/k_B T)}{g_1 g_0 \psi (1-\psi)} [1+\exp(-\zeta/k_B T)] \times \{1+\exp[(-\epsilon+\lambda\psi+\zeta)/k_B T]\} , \tag{50}$$

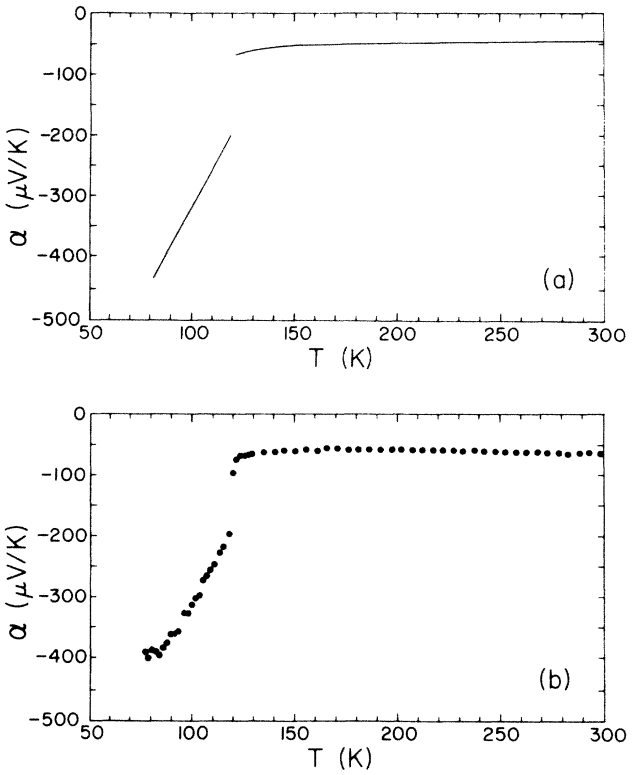

FIG. 5. Seebeck coefficient (α): (a) calculated and (b) experimental (Ref. 26).

which groups the inverse of all temperature-dependent factors of Eq. (49), where ψ, ϵ, and ζ can be calculated from Eqs. (5), (36), and (41), respectively. Logarithmic plots of R versus dc electrical resistivity[26] of stoichiometric ($\delta=0$) magnetite above [see Fig. 6(a)] and below [see Fig. 6(b)] the Verwey transition show that, below T_V, the experimental resistivity approaches the straight line of unity slope expected for adiabatic behavior, whereas a marked departure exists above T_V. This result is consistent with the experimental[28] observation that the ac resistivity is frequency dependent above, but not below, T_V.

The calculated R and experimental ρ values at room temperature may be used to evaluate ν_o, by substitution of the appropriate constants in Eq. (49), with the result $\nu_o \simeq 10^{13}$, which is the order of magnitude[29] for polaronic effects in the $3d$ states of transition-metal oxides. A similar calculation yields $\nu_o \simeq 10^{10}$, for the ordered structure below T_V, simulating the softening of the mode.[30]

The usual logarithmic plots of resistivity as a function of inverse temperature for experimental and calculated values in stoichiometric magnetite are shown in Fig. 7. A direct temperature plot (see Fig. 8) reveals that the calculated resistivity displays the shallow minimum at 360 K, characteristic of the experimental data.[31]

VI. DISCUSSION

The results of systematic experimental investigations of the Verwey transition in $Fe_{3(1-\delta)}O_4$, as a function of nonstoichiometry (δ), have been interpreted in terms of a simple mean-field model. It has been shown that the diffeomorphism, which maps the critical manifold to the cusp-catastrophe characteristic of the mean-field approximation, depends on the degeneracies of the relevant states of the microsystems. The appropriate degeneracy schemes are dictated by thermodynamic relations, rather than by specific models of the microstates. The resulting criticality is a function of the magnitude of an internal energy parameter, which subsumes all interactions between subsystems, linearly related to composition by the change of the $[Fe^{2+}]/[Fe^{3+}]$ ratio.

It has not escaped the authors' attention that various descriptions of the subsystems, including elementary crystal-field models, can account for the assigned degeneracies. It was deemed preferable, however, to preserve the integrity of the thermodynamic treatment, refraining from assumptions on the nature of the microstates. Hence, the scope and limitations of this work are those of the mean-field approximation employed. In this perspective, it is clear that the critical exponent value, $\frac{1}{2}$, arises as a consequence of identifying the average state of the system with the most probable one, and requires renormalization techniques for further investigation. Similarly, the long-range-order parameter ψ has been

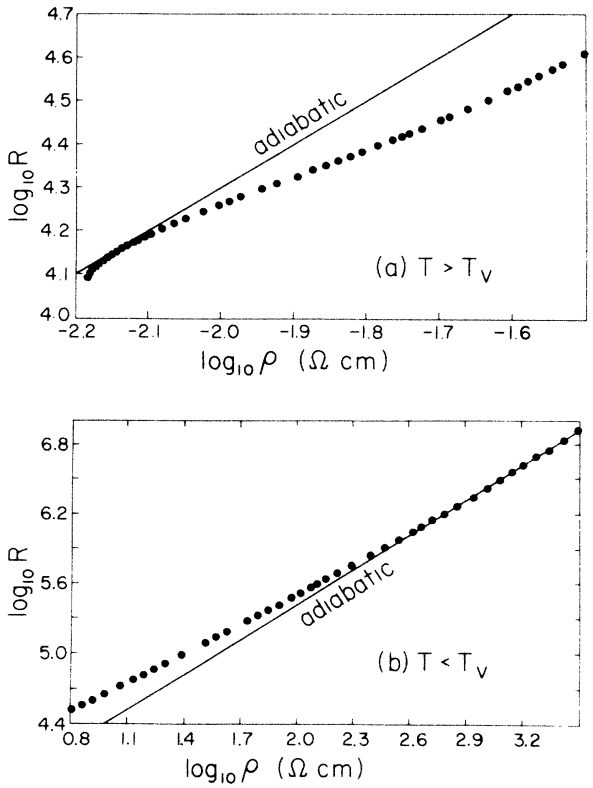

FIG. 6. Logarithmic plot of the temperature-dependent part of resistivity (R), calculated in the adiabatic small-polaron approximation, vs the experimental (Ref. 34) dc electrical resistivity (ρ), (a) above and (b) below the Verwey transition. Unity slope line is the reference adiabatic limit.

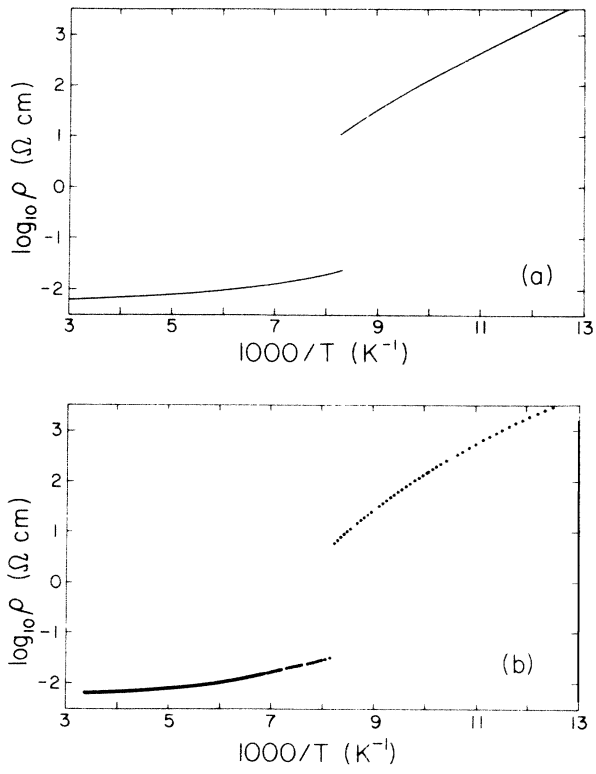

FIG. 7. Logarithm of dc electrical resistivity vs inverse temperature (a) calculated in the adiabatic small-polaron approximation, and (b) experimental (Ref. 26).

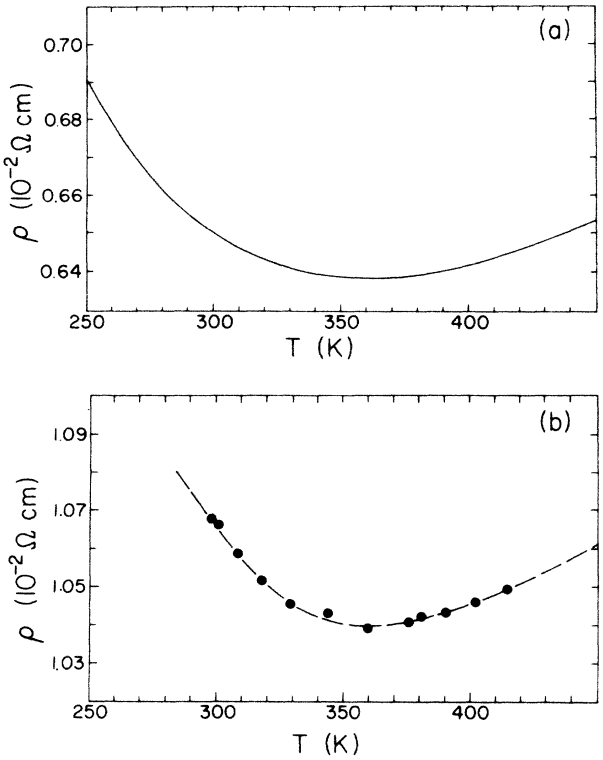

FIG. 8. dc electrical resistivity vs temperature (a) calculated in the adiabatic small-polaron approximation, and (b) experimental (Ref. 31).

treated as a scalar, which precludes any attempt to describe anisotropic behavior. However, higher dimensionality of ψ will not change the physics, unless different functionals of the ϵ and λ parameters are introduced. Finally, although it is clear that any externally induced change in the ϵ/λ ratio would alter critical behavior, the investigation of possible symmetry-breaking terms also requires additional information on the subsystems.

These considerations extend quite naturally to the interpretation of the physical properties of magnetite. The description of electrical transport has shown that, with the use of a single long-range-order parameter to account for the thermal dependence of the density of states, the main features of electrical resistivity and Seebeck-coefficient measurements can be interpreted with nothing more elaborate than an elementary small-polaron model. The need for additional characterization of the microstates arises whenever knowledge of the initial and final states of electron transfer is required, such as in the evaluation of nonadiabatic terms or of specific scattering mechanisms. Even then, the equilibrium treatment defines the limits for application of intrinsic conduction models. Since the conductivity is proportional to the square of the order parameter [see Eq. (49)], it is clear that below liquid-N_2 temperatures, for $\psi < 0.01$, the impurity content of even the best available samples contributes significantly to electrical transport.

ACKNOWLEDGMENTS

The authors are indebted to R. Rasmussen for a careful review of the manuscript. This work was supported by the National Science Foundation under Grant No. DMR-86-16533.

APPENDIX

The pertinent theorem, proved by Magnus, as cited in Ref. 8, states that "A versal unfolding F of f is strongly equivalent to the truncated unfolding

$$j^p f(x) + t_1 J^q \left[\frac{\partial}{\partial t_1} F_{t_1,0,\ldots,0} \right] + \cdots + t_r J^q \left[\frac{\partial}{\partial t_r} F_{0,\ldots,0,t_r} \right], \quad \text{(A1)}$$

if f is strongly k determinate, $k \geq 3$." It has been applied here in the first of the possible cases: "$M_n^{k-1} \subseteq \Delta_{k+1}(f)$, with $p \geq 2k-3$ and $q \geq k-2$." j^k is the Taylor expansion to order k, J^k is j^k minus its constant term, and the t_i are the control variables; M_m^k is the vector space of homogeneous polynomials in n variables of degree k and Δ_k the subspace of J_n^k spanned by $Qj^k(\partial f/\partial x_i)^{\bar{k}}$.

[1]E. J. Verwey and P. W. Haajman, Physica (Utrecht) **8**, 979 (1941).

[2]R. Aragón, D. J. Buttrey, J. P. Shepherd, and J. M. Honig, Phys. Rev. B **31**, 430 (1985).

[3]J. P. Shepherd, Ph. D. thesis, Purdue University, 1984; J. P. Shepherd, R. Aragón, J. W. Koenitzer, and J. M. Honig, Phys. Rev. B **32**, 1818 (1985); R. Aragón, J. P. Shepherd, J. W. Koenitzer, D. J. Buttrey, R. J. Rasmussen, and J. M. Honig, J. Appl. Phys. **57**, 3221 (1985).

[4]W. T. Grandy, in *Structural Stability in Physics*, edited by W. Guttinger and H. Eikemeier (Springer-Verlag, Berlin, 1979).

[5]S. Strässler and C. Kittel, Phys. Rev. **139**, A758 (1965).

[6]Generalizations to multiple states have been attempted; see, for instance, V. M. Talanov and G. V. Bezrukov, Phys. Status Solidi A **96**, 475 (1986).

[7]Not to be confused with the variable of the same name used in Ref. 5 for the transition temperature, identified here by T_V.

[8]T. Poston and I. Stewart, *Catastrophe Theory and its Applications* (Pitman, London, 1978), p. 339.

[9]*Catastrophe Theory and its Applications*, Ref. 8, p. 134, theorem 8.1.

[10]*Catastrophe Theory and its Applications*, Ref. 8, p. 153, theorem 8.7. Also see the Appendix.

[11]The appropriate form of the truncated unfolding defined in the Appendix is

$$jf(r) + eJ^1 \left[\frac{\partial}{\partial e} F_{e,0} \right] + 1J^1 \left[\frac{\partial}{\partial 1} F_{0l} \right].$$

[12]The appropriate form of the truncated unfolding defined in

the Appendix is

$$J^5(\Phi_{0,0})+J^2\left[\frac{\partial}{\partial e}\Phi_{e,0}\right]+J^2\left[\frac{\partial}{\partial l}\Phi_{0l}\right] .$$

[13]*Catastrophe Theory and its Applications,* Ref. 8, p. 99.

[14]See, for instance, J. G. Dubois and J. P. Dufour, Annu. Inst. Henri Poincaré, A **29**, 1 (1978), for proof of the equivalence of Legendre and catastrophe invariances.

[15]Numerous monographs describe the cusp catastrophe in detail. See, for instance, *Catastrophe Theory and its Applications,* Ref. 8, pp. 78 and 174.

[16]*Catastrophe Theory and its Applications,* Ref. 8, p. 327; D. H. Fowler, in *Towards a Theoretical Biology,* edited by C. H. Waddington (Edinburgh University Press, Edinburgh, 1968–1972), Vol. 4, p. 1.

[17]*Catastrophe Theory and its Applications,* Ref. 8, p. 352.

[18]*Catastrophe Theory and its Applications,* Ref. 8, p. 331.

[19]L. D. Landau and E. M. Lifshitz, *Statistical Physics* (Pergamon, Oxford, 1959), p. 434.

[20]*Catastrophe Theory and its Applications,* Ref. 8, p. 338.

[21]J. P. Shepherd, J. W. Koenitzer, R. Aragón, C. J. Sandberg, and J. M. Honig, Phys. Rev. B **31**, 1107 (1985).

[22]D. B. Chesnut, J. Chem. Phys. **40**, 405 (1964).

[23]*Catastrophe Theory and its Applications,* Ref. 8, p. 389.

[24]D. Emin, Philos. Mag. **51**, L53 (1985).

[25]D. Emin, Phys. Rev. B **30**, 5766 (1984).

[26]R. J. Rasmussen, R. Aragón, and J. M. Honig, J. Appl. Phys. **61**, 4395 (1987), and recent unpublished Seebeck-coefficient measurements.

[27]See, for instance, H. L. Tuller and A. S. Norwick, J. Phys. Chem. Solids **38**, 859 (1977).

[28]R. Rasmussen (private communication).

[29]J. G. Austin and N. F. Mott, Science **168**, 70 (1970).

[30]The softening of the Δ_5 phonon mode has been the subject of numerous investigations. See, for instance, M. Izumi and G. Shirane, Solid State Commun. **17**, 433 (1975).

[31]C. A. Domenicali, Phys. Rev. **78**, 458 (1950).